Available online at www.sciencedirect.com

SciVerse ScienceDirect

Ceramics International 39 (2013) 6861–6866

CERAMICS INTERNATIONAL

www.elsevier.com/locate/ceramint

Graphene supported poly-pyrrole(PPY)/Li_2SnO_3 ternary composites as anode materials for lithium ion batteries

Yang Zhao, Ying Huang*, Qiufen Wang

Department of Applied Chemistry and The Key Laboratory of Space Applied Physics and Chemistry, Ministry of Education, School of Science, Northwestern Polytechnical University, Xi'an 710072, PR China

Received 25 January 2013; received in revised form 7 February 2013; accepted 8 February 2013
Available online 14 February 2013

Abstract

The GNS/Li_2SnO_3/PPY ternary composites were synthesized by a deoxidation technique. The soft polymer matrix and flexible graphene provide a dual buffering structure for Li_2SnO_3 which synergistic leads to improved stability, enhanced electric conductivity and better electrochemical performance. The GNS/Li_2SnO_3/PPY composites tested as anode materials for lithium ion batteries exhibit a high reversible capacity of 699.4 mAh/g over 30 cycles, which is much better than that of pure Li_2SnO_3, PPY/Li_2SnO_3 and GNS/Li_2SnO_3 composites.

Keywords: Graphene/Li_2SnO_3/poly-pyrrole ternary composites; Lithium ion batteries; Electrochemical properties

1. Introduction

The lithium ion battery is considered to be an excellent portable electronic product and electric vehicle power supply due to its small size and high energy density [1]. At present, graphite is widely used as an anode material for lithium ion batteries, but its relatively low theoretical capacity (372 mAh/g) limits further applications [2]. To improve the energy density, cycling life and high-rate capability, much effort has been prompted to develop novel electrode materials. Among the large number of alternative anode materials, tin-based materials have received researchers' attention, owing to their high theoretical capacities [3]. Li_2SnO_3, a kind of NaCl-type Tin-based metal salt, has attracted more interest of the researchers for its great potential [4]. However, this kind of Tin-based anode materials suffers from the poor cycling performance owing to the large volume changes and nanoparticle aggregation during Li insertion/extraction processes [5–7].

Conducting polymers, such as poly-aniline(PANI) and poly-pyrrole(PPY), thought as good to improve the electrode properties can provide buffer structures for the active materials [8]. Moreover, conducting polymer/inorganic oxide nanocomposites have attracted great attention because of their unique structure [9], microwave absorption properties [10], and especially the wide range of potential uses as a battery anode [11–13].

Graphene is of interest due to its unique structure, high specific surface area, and superior electronic conductivity [14]. The unique two-dimensional structure of graphene with a high specific surface area and abundant functional groups can be a relatively stable carrier [15–17]. The accession of graphene can effectively alleviate the serious volume expansion of the anode material in the process of lithium intercalation and deintercalation, while creating synergies with active materials, which contributes to a higher specific capacity and better cycling performance than the original materials [18].

In this paper, we report a new ternary GNS/ Li_2SnO_3/PPY composite material. The addition of PPY and graphene can create a double buffer structure for Li_2SnO_3. The GNS/ Li_2SnO_3/PPY composites show superior electrochemical performance than the binary and original materials.

*Corresponding author. Tel.: +86 29 88431636.
E-mail addresses: zhaoyang890@163.com (Y. Zhao), yingh@nwpu.edu.cn (Y. Huang).

0272-8842/$ - see front matter © 2013 Elsevier Ltd and Techna Group S.r.l. All rights reserved.
http://dx.doi.org/10.1016/j.ceramint.2013.02.020

2. Experimental

2.1. Sample preparation

Li_2SnO_3 and Li_2SnO_3/PPY composites were synthesized based on our previous research via a hydrothermal process [19] and a micro emulsion polymerization [13]. Graphite oxide (GO) was prepared with a modified Hummers method [20].

GO (0.5057 g) and the as-prepared Li_2SnO_3/PPY (1.5104 g) were dispersed in the dimethylformamide (DMF, 250 ml), respectively, followed by ultrasonication for dispersion. Li_2SnO_3/PPY-DMF solution was slowly added into the GO-DMF solution and stirred for 1 h, then $N_2H_4 \cdot H_2O$ (2 ml, 30%) was mixed with the solution and stirred at 95 °C for 24 h. When the solution temperature decreased, the samples were filtered, and subsequently washed with deionized water and ethanol, followed by drying at room temperature as the GNS/Li_2SnO_3/PPY composites.

2.2. Materials characterization

The structure of the prepared samples was characterized by X-ray diffraction analysis (XRD) (Rigaku, model D/max-2500 system at 40 kV and 100 mA of Cu K). The Raman spectra of the composite samples were obtained using an inVia Laser-Raman spectrometer (Renishaw Co., England) with a 514 nm radiation. The surface morphology study of the composite was performed by model Tecnai F30 G2 (FEI Co., USA) field emission transmission electron microscope (FETEM). Thermal analysis of the composite was performed by thermal gravimetric analysis (TGA) (Model Q50, TA, USA) under an air atmosphere, with a heating rate of 20 °C/min, and the temperature range was from 20 °C to 700 °C. The Fourier transform infrared spectroscopy (FTIR) spectras were obtained by using a Model NIcolETiS10 Fourier transform spectrometer (Thermo SCI-ENTIFIC Co., USA) with a 2 cm^{-1} resolution in the range of 400–4000 cm^{-1}.

The anode electrodes were prepared by coating slurries consisting of GNS/Li_2SnO_3/PPY composites (65 wt.%) with acetylene black (15 wt.%) and PVDF (20 wt.%) as a binder dissolved in 1-methyl-2-pyrrolidinone (NMP) solution on a copper foil. Electrochemical performance was tested in a CR2016-type coin cell by a multi-channel current static system Land (LAND CT200IA) using metallic Li foil as counter electrode and polypropylene (PP) film (Celgard 2400) as separator. The electrolyte was a solution of 1 M $LiPF_6$ in a mixture of ethylene (EC), dimethyl carbonate (DMC) and diethyl carbonate (DEC) (1:1:1, v/v/v). Cyclic voltammetry (CV) was performed on a Series G 750™ Redefining Electrochemical Measurement (USA GMARY Co.).

3. Results and discussion

Fig. 1(a) shows the XRD patterns of the as-prepared Li_2SnO_3/PPY and GNS/Li_2SnO_3/PPY composites. The diffraction peaks of crystalline Li_2SnO_3 nanoparticles are clearly distinguishable in the both patterns. The peaks of the PPY and graphene have not been obviously observed due to their little content and non-crystalline structure. All strong diffraction lines can be indexed to the standard monoclinic Li_2SnO_3 phase (PDF#31–0761), indicating the strong crystalline nature of the Li_2SnO_3. The standard data of Li_2SnO_3 monoclinic crystal structure with lattice constants is about $a=5.301$ Å, $b=9.181$ Å, and $c=10.027$ Å. The XRD analysis shows that the crystal structure of Li_2SnO_3 has not been changed after the addition of PPY and graphene.

The FITR spectrums of the Li_2SnO_3/PPY and GNS/Li_2SnO_3/PPY composites are shown in the Fig. 1(b). The strong vibration at about 520 cm^{-1} is seen in the low wave number region corresponding to the Sn–O vibration mode of Li_2SnO_3. The absorption at around 1560 cm^{-1} can be assigned to the stretching vibration of C=C in the the pyrrole rings, while the characteristic peaks at 1650 cm^{-1} and 1110 cm^{-1} are related to C=C ring skeletal stretching and C–H in-plane vibrations., respectively [18]. The band at 929 cm^{-1} can be assigned to N–H in-plane vibrations. The peak at 3400 cm^{-1} can be attributed to the O–H stretching vibrations of the structural −OH groups [21]. Compared with the Li_2SnO_3/PPY composites, it can be observed that most of the marked peaks are shifted left when the graphene was added into the composites. This reveals that the groups from the graphene are associated to the nitrogenous functional groups of PPY backbone [22]. Herewith, there probably exist interactions between PPY and graphene such as π-π nocovalent bonds or hydrogen bonding for the residual oxygen functional groups on graphene [23].

Fig. 1(c) shows the Raman shifts of Li_2SnO_3/PPY and GNS/Li_2SnO_3/PPY. The peak at about 1592 cm^{-1} (G band) is related to the vibration of sp2-bonded carbon atoms in a 2-dimensional hexagonal lattice, while the 1334 cm^{-1} peak (D band) could be related to the defects and disorder in the hexagonal graphitic layers [24]. There is a broad peak at about 1000 cm^{-1}, which is the characteristic peak of PPY [22]. The G band is much higher than the D band after the addition of the graphene likely due to the π-π nocovalent between PPY and graphene.

Fig. 1(d) display the TGA curves of the two samples that characterize in air. A gradual weight loss occurs between 100 °C and 600 °C, indicating the oxidation and decomposition of graphene and PPY in air. Therefore, the change in weight before and after the oxidation of graphene or PPY can be transformed into the amount of graphene or PPY in the materials, respectively. As can be seen from the TGA curves, the mass fraction of PPY in the Li_2SnO_3/PPY is about 15 wt%, demonstrating about 10 wt% graphene contained in GNS/Li_2SnO_3/PPY.

As shown in the Fig. 2(a), Li_2SnO_3/PPY nanocomposites are supported by the flexible graphene nanosheets, which can provide the double buffering structure for the GNS/Li_2SnO_3/PPY composite. It also can be seen that

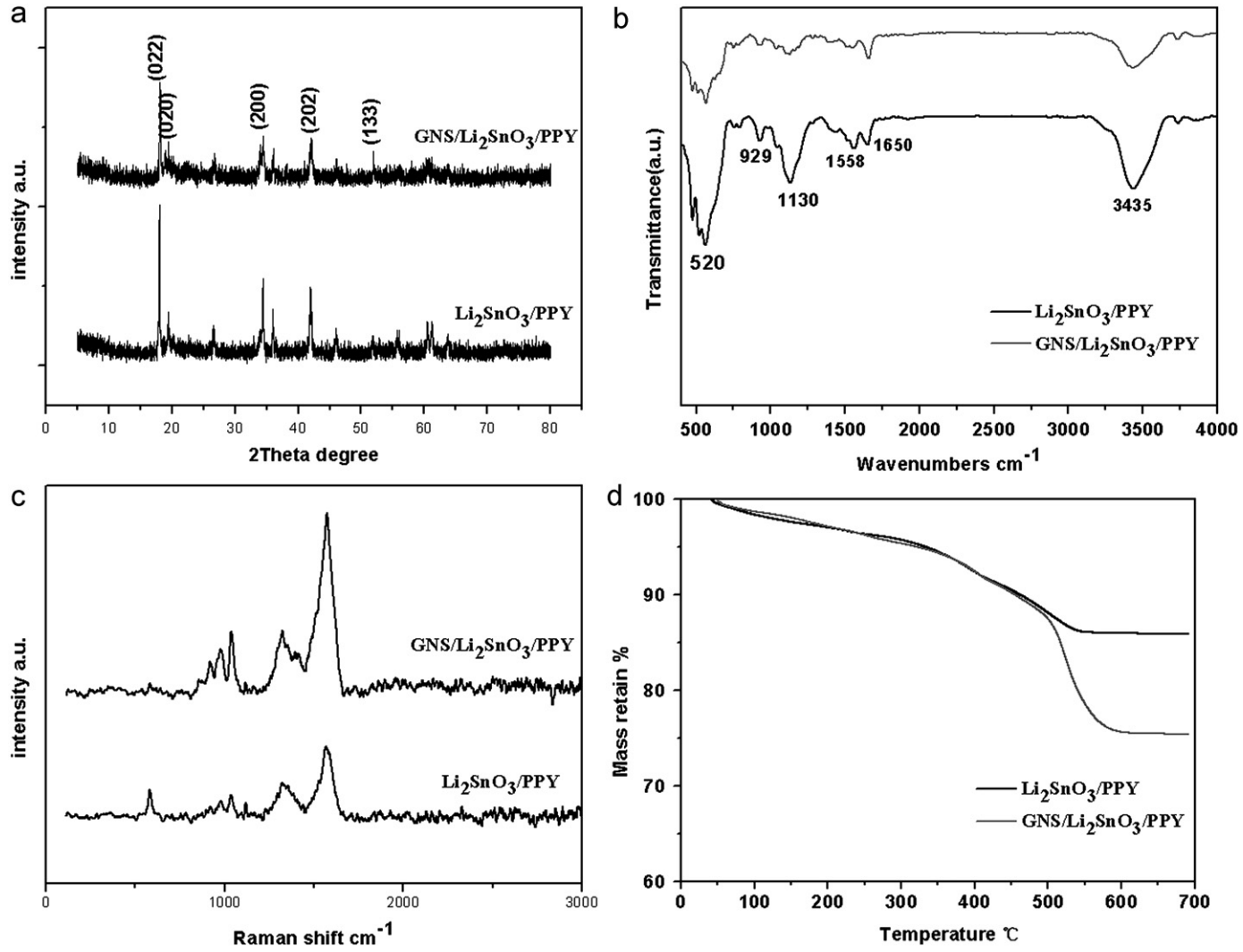

Fig. 1. The XRD patterns (a), FTIR spectrums (b), Raman shifts (c), TGA curves (d) of the Li_2SnO_3/PPY composites and GNS/Li_2SnO_3/PPY composites.

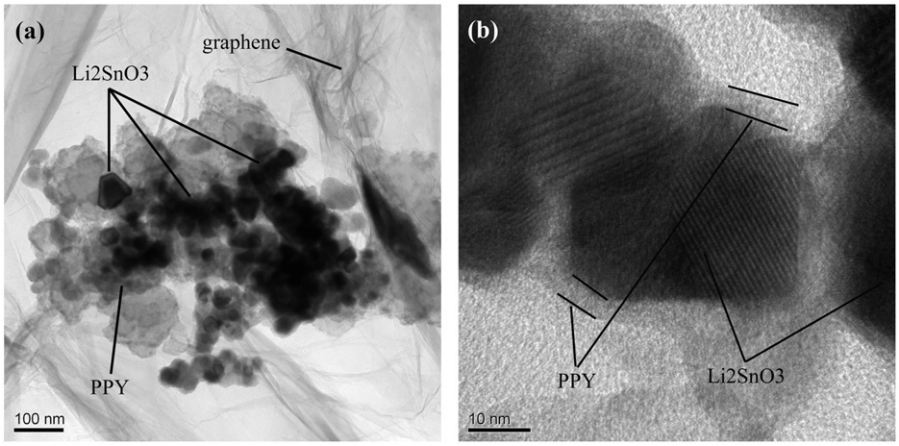

Fig. 2. TEM images of as prepared GNS/Li_2SnO_3/PPY composites(a, b).

Li_2SnO_3 nanocrystallites are homogeneously distributed in the PPY matrix to form the Li_2SnO_3/PPY composites. From the HR-TEM (b) of the partial enlarged GNS/Li_2SnO_3/PPY composite, Li_2SnO_3 nanoparticles have the clear lattice fringes and there is no obvious lattice structure in the PPY matrix. The soft polymer matrix and

flexible graphene may show the function of accommodating the internal stress of anodes that suffer from severe volume change [25]. The PPY/Li_2SnO_3 nanoparticles may be combined with graphene via Van der Waals force. There are abundant functional groups on the surface of graphene and the composites. From the FITR spectrums and Raman shifts, the composites may show the stability with the π–π noncovalent between PPY and graphene. In addition, the PPY/Li_2SnO_3 nanoparticles are distributed on the surface of few layers graphene sheets as the TEM images in Fig. 2(a,b). The PPY/Li_2SnO_3 nanoparticles are separated and supported by the stacked graphene sheets. So the structures of the composites are stable. In summary, the intermolecular forces and the specific structure can prevent the detaching of the composites.

The electrochemical properties of the GNS/Li_2SnO_3/PPY composite are illustrated in Fig. 3. The charge–discharge curves of the 1st and 2nd cycles are displayed in Fig. 3(a). The discharge capacity and charge capacity of the composite are 1465 mAh/g and 771 mAh/g in the first cycle, respectively. The large irreversible capacity after the first cycle for the composites has gone away due to the severe side reaction forming solid electrolyte interphase (SEI) film and the loss of Li_2SnO_3.

The electrochemical reactivity of the anode in lithium ion battery is evaluated by cyclic voltammetry (CV). Fig. 3 shows the *CV* curves of GNS/Li_2SnO_3/PPY composites from the first to the 7th cycles. In the first cycle, there is a cathodic peak at 0.02 V, which can be attributed to the formation of the solid electrolyte interphase (SEI) layer. However, this peak disappears in the following cycles. From the second to the 7th cycle, the anodic peak at 0.2 V corresponds to lithium insertion with graphene and the alloying of LixSn; the cathodic peak at 0.6 V can be assigned to the extraction of lithium from graphene and de-alloying of LixSn [18].The weak cathodic peak at 1.25 V and the similar anodic peak at 0.8 V may result from the reversible reaction between Sn and Li_2O [26].

To evaluate the rate performance of the GNS/Li_2SnO_3/PPY composites, the charge/discharge measurements are carried out at various current densities in Fig. 3(c). At a current density of 60 mA/g, the discharge (charge) capacities of the GNS/Li_2SnO_3/PPY composites can remain about 699.4 (684.3) mAh/g. With the current density increased to 120 mA/g, 180 mA/g, 300 mA/g, 600 mA/g, the composites still can deliver a discharge(charge) capacity of 656.1(6 4 0) mAh/g, 579.2(563.2) mAh/g, 493(487.7)

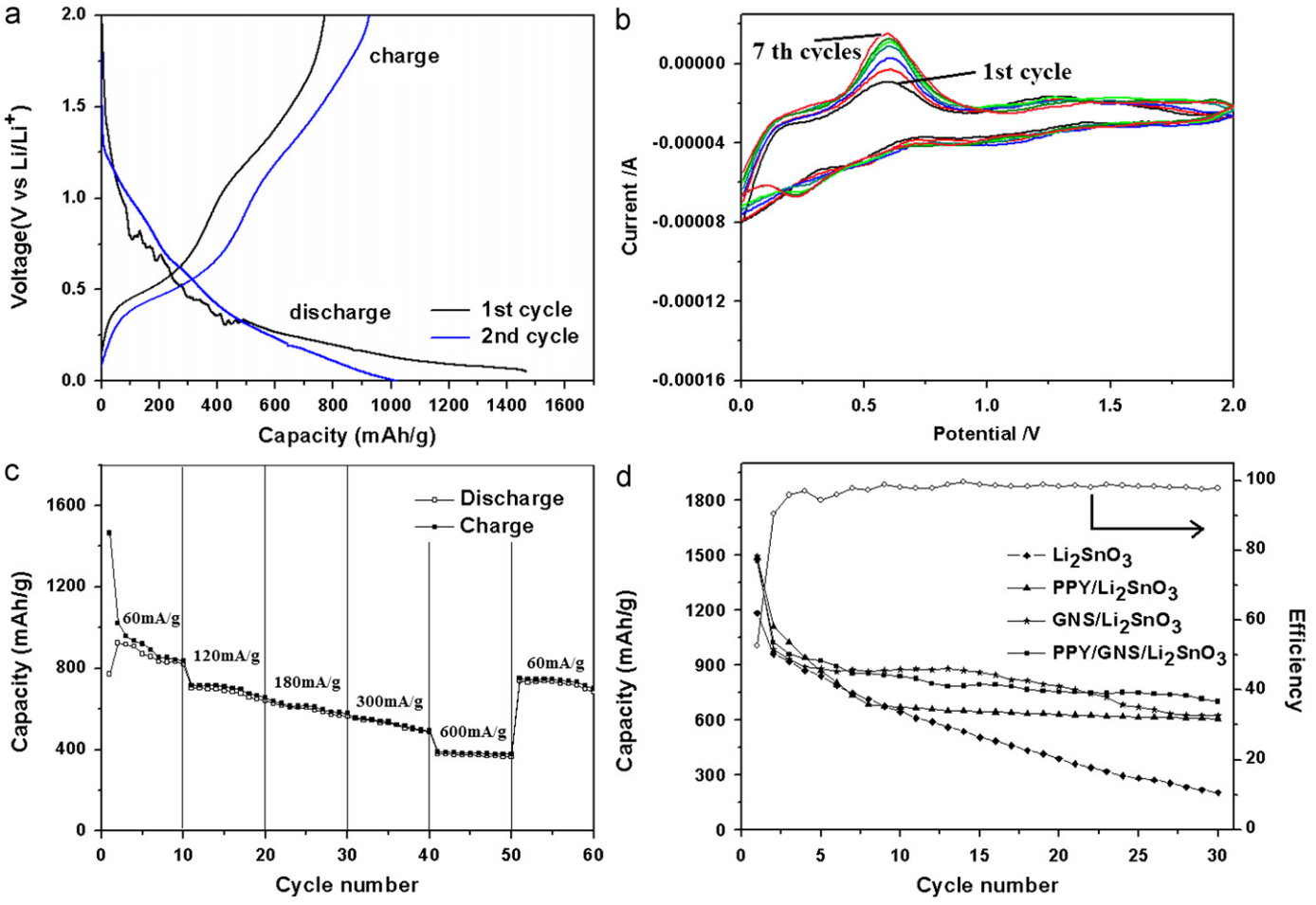

Fig. 3. The first and second cycle charge–discharge voltage profiles (a), the cyclic voltammetry curves (b), the rate capacities and (c) the cyclic performance for the GNS/Li_2SnO_3/PPY composites.

mAh/g and 377.9(366.2) mAh/g up to 30 cycles, respectively. Despite the capacity fading of the composite declined largely at high rates, the anode still exhibit an excellent cycling performance, indicating that the double buffering structure is effective.

As observed in Fig. 3(d) regarding galvanostatic charge/discharge cycling results, the Li_2SnO_3 anode yields a reversible specific capacity of around 956.3 mAh/g at a current density of 60 mA/g. However, the capacity drops dramatically to 202 mAh/g at the 30th cycle. The reversible specific capacity of PPY/Li_2SnO_3 and GNS/Li_2SnO_3 composites is 605 mAh/g and 622 mAh/g at the 30th cycle, respectively. In contrast, the GNS/Li_2SnO_3/PPY composite shows a better cycling performance and the reversible capacity is 699.4 mAh/g at the 30th cycle. A stable coulombic efficiency of 95% has been achieved since the third cycle. These results may be due to the double buffering structure provided by PPY and graphene. This structure can accommodate the large volume change of Li_2SnO_3 anode materials during Li+ insertion/extraction and restraint the cracking of composite electrodes, resulting in an enhanced cycling performance.

4. Summary

The GNS/Li_2SnO_3/PPY ternary composites as anode materials for lithium ion batteries are prepared via a deoxidation method. In this way, the Li_2SnO_3 nanoparticles are in the dual buffering structure of PPY and graphene contributing to less volume expansion of Li_2SnO_3 anode. The composites show good rate performances with achieving a reversible capacity of 699.4 mAh/g after 30 cycles. The high Li-storage performance, cycling coulombic efficiency and low capacity loss of the ternary composites are better than those of the original Li_2SnO_3 and two other binary materials. Therefore, the composites reported here are very promising anode materials for the future development of lithium ion batteries.

Acknowledgments

This work was supported by the Spaceflight Foundation of the People's Republic of China under Grant no. N8XW0002. This work was supported by the Graduate Starting Seed Fund of Northwestern Polytechnical University No. Z2013146.

References

[1] C.F. Li, W.H. Ho, C.S. Jiang, C.C. Lai, M.J. Wang, S.K. Yen, Electrolytic Sn/Li_2O coatings for thin-film lithium ion battery anodes, Journal of Power Sources 196 (2011) 768–775.

[2] Y.X. Wang, L. Huang, Y.Q. Chang, F.S. Ke, J.T. Li, S.G. Sun, Fabrication and electrochemical properties of the Sn–Ni–P alloy rods array electrode for lithium-ion batteries, Electrochemistry Communications 12 (2010) 1226–1229.

[3] L. Jose, Tirado, Inorganic materials for the negative electrode of lithium-ion batteries: state-of-the-art and future prospects, Materials Science and Engineering 40 (2003) 103–136.

[4] D.W. Zhang, S.Q. Zhang, Y. Jin, T.H. Yi, S. Xie, C.H. Chen, Li_2SnO_3 derived secondary Li–Sn alloy electrode for lithium-ion batteries, Journal of Alloys and Compounds 415 (2006) 229–233.

[5] Q.Y. Li, S.J. Hu, H.Q. Wang, F.P. Wang, X.X. Zhong, X.Y. Wang, Study of copper foam-supported Sn thin film as a high-capacity anode for lithium-ion batteries, Electrochimica Acta 54 (2009) 5884–5888.

[6] X.J. Zhu, Z.P. Guo, P. Zhang, G.D. Du, C.K. Poh, Z.X. Chen, S. Li, H.K. Liu T, Three-dimensional reticular tin–manganese oxide composite anode materials for lithium ion batteries, Electrochimica Acta 55 (2010) 4982–4986.

[7] K.E. Aifantis, S. Brutti, S.A. Hackney, T. Sarakonsri, B. Scrosatie, SnO_2/C nanocomposites as anodes in secondary Li-ion batteries, Electrochimica Acta 55 (2010) 5071–5076.

[8] L. Yuan, J. Wang, S.Y. Chew, J. Chen, Z.P. Guo, L. Zhao, K. Konstantinov, H.K. Liu, Synthesis and characterization of SnO_2–polypyrrole composite for lithium-ion battery, Journal of Power Sources 174 (2007) 1183–1187.

[9] M.R. Mahmoudian, W.J. Basirun, Y. Alias, M. Ebadi, Synthesis and characterization of polypyrrole/Sn-doped TiO_2 nanocomposites (NCs) as a protective pigment, Applied Surface Science 257 (2011) 8317–8325.

[10] Y. Wang, Y. Huang, Q.F. Wang, Q. He, L. Chen, Preparation and electromagnetic properties of Polyaniline(polypyrrole)–$BaFe_{12}O_{19}$/$Ni_{0.8}Zn_{0.2}Fe_2O_4$ ferrite nanocomposites, Applied Surface Science 259 (2012) 486–493.

[11] Z.J. Du, S.C. Zhang, T. Jiang, X.M. Wu, L. Zhang, H. Fang, Facile synthesis of SnO_2 nanocrystals coated conducting polymer nanowires for enhanced lithium storage, Journal of Power Sources 219 (2012) 199–203.

[12] H.Y. Mi, Y.L. Xu, W. Shi, H.D. Yoo, S.J. Park, Y.W. Park, S.M. Oh, Polymer-derived carbon nanofiber network supported SnO_2 nanocrystals: a superior lithium secondary battery material, Journal of Materials Chemistry 21 (2011) 19302–19309.

[13] Q.F. Wang, Y. Huang, J. Miao, Y. Zhao, Y. Wang, Synthesis and properties of Li_2SnO_3/polyaniline nanocomposites as negative electrode material for lithium-ion batteries, Applied Surface Science 258 (2012) 9896–9901.

[14] A.K. Geim, Graphene: status and prospects, Science 324 (2009) 1530–1534.

[15] P.C. Lian, X.F. Zhu, S.Z. Liang, Z. Li, W.S. Yang, H.H. Wang, High reversible capacity of SnO_2/graphene nanocomposite as an anode material for lithium-ion batteries, Electrochimica Acta 56 (2011) 4532–4539.

[16] R.M. Iresha, N.H. Kottegoda, L. Idris, J.Z. Lu, H.K. Wang, Liu, Synthesis and characterization of graphene–nickel oxide nanostructures for fast charge–discharge application, Electrochimica Acta 56 (2011) 5815–5822.

[17] J.S. Zhou, L.L. Ma, H.H. Song, B. Wu, X.H. Chen, Durable high-rate performance of CuO hollow nanoparticles/graphene-nanosheet composite anode material for lithium-ion batteries, Electrochemistry Communications 13 (2011) 1357–1360.

[18] Y. Zhao, Y. Huang, Q.F. Wang, X.Y. Wang, M. Zong, Carbon-doped Li_2SnO_3/graphene as highly reversible an anode material for lithium-ion batteries, Ceramics International, 39(2013) 1741.

[19] Q.F. Wang, Y. Huang, J. Miao, Y. Wang, Y. Zhao, Hydrothermal derived Li_2SnO_3/C composite as negative electrode materials for lithium-ion batteries, Applied Surface Science 258 (2012) 6923–6929.

[20] L.J. Wan, Z.Y. Ren, H. Wang, G. Wang, X. Tong, S.H. Gao, J.T. Bai, Graphene nanosheets based on controlled exfoliation process for enhanced lithium storage in lithium-ion battery, Diamond and Related Materials 20 (2011) 756–761.

[21] B. Zhao, G.H. Zhang, J.S. Song, Y. Jiang, H. Zhuang, P. Liu, T. Fang, Bivalent tin ion assisted reduction for preparing graphene/SnO_2

composite with good cyclic performance and lithium storage capacity, Electrochimica Acta 56 (2011) 7340–7346.

[22] D. Zhang, X. Zhang, Y. Chen, P. Yu, C.H. Wang, Y.W. Ma, Enhanced capacitance and rate capability of graphene/polypyrrole composite as electrode material for supercapacitors, Journal of Power Sources 196 (2011) 5990–5996.

[23] C.F. Zhang, X. Peng, Z.P. Guo, C.B. Cai, Z.X. Chen, D. Wexler, Carbon-coated SnO_2/graphene nanosheets as highly reversible anode materials for lithium ion batteries, Carbon 50 (2012) 1897–1903.

[24] S. Bose, T. Kuila, M.E. Uddin, N.H. Kim, A.K.T. Lau, J.H. Lee, In-situ synthesis and characterization of electrically conductive polypyrrole/graphene nanocomposites, Polymer 51 (2010) 5921–5928.

[25] L.F. Cui, J. Shen, F.Y. Cheng, Z.L. Tao, J. Chen, SnO_2 nanoparticles@polypyrrole nanowires composite as anode materials for rechargeable lithium-ion batteries, Journal of Power Sources 196 (2011) 2195–2201.

[26] I.A. Courtney, J.R. Dahn, Key factors controlling the reversibility of the reaction of lithium with SnO_2 and Sn_2BPO_6 glass, Journal of the Electrochemical Society 144 (1997) 2943–2948.